Surface chemistry in Atomic Layer Deposition of Gallium Nitride from Triethylgallium and Ammonia studied by mass spectroscopy

Houyem Hafdi*, Pamburayi Mpofu, Alex Moberg Byam, Henrik Pedersen*

Department of Physics, Chemistry and Biology, Linköping University, SE-581 83, Linköping, Sweden

*Corresponding author: houyem.hafdi@liu.se, henrik.pedersen@liu.se

Gallium nitride (GaN) is a commonly used semiconductor owing to its high chemical and thermal stability, which makes it suitable for various applications in modern electronics. GaN film deposition is favored by atomic layer deposition (ALD) with triethylgallium (TEG) and ammonia (NH_3) plasma as precursors. However, the surface reaction pathways of TEG under ALD conditions have not been experimentally evaluated. In this study, the surface chemistry of GaN films deposited on Si (100) during ALD with TEG and NH_3 with and without plasma activation as precursors was investigated using mass spectrometry. The results suggest that the surface chemistry of the deposition process mainly consists of ethyl ligand elimination upon the TEG pulse, followed by ligand exchange during NH_3 pulsing to form ethane (C_2H_6) as a reaction by-product on an NH_2-terminated surface.

I. INTRODUCTION

Gallium Nitride (GaN) is an important wide-gap (3.4 eV) semiconductor with applications in opto- and power electronics.[1] It offers excellent chemical durability and a high breakdown field strength.[2] The high optical transparency and chemical stability of GaN make it a suitable material for solar cells.[3] All of these applications require the deposition of GaN thin layers or films. An emerging technique for thin GaN films is atomic layer deposition (ALD), a technique based on sequential delivery of gaseous reactant molecules to the surface of a heated substrate where surface chemical reactions deposit, ideally, one atomic layer. The film growth self-limits after the chemical reactions have consumed all available surface sites. The reactor is then purged before introducing the subsequent precursor onto the substrate to deposit a layer of a second type of atoms[4]. The most common gallium precursors are the tri-alkyl metal molecules, trimethylgallium (TMG), and triethylgallium (TEG)[5,6], and Ammonia (NH_3), with or without plasma activation, or nitrogen plasma, are common nitrogen precursors. It has been shown that GaN deposited using TMG exhibits better optical and structural properties than GaN deposited using TEG.[7] The very high vapor pressure of TMG makes it challenging to use in ALD, where the precursor vapor is typically drawn by low pressure in the reactor.[8] Therefore, the use of TMG requires either valves that can open for a very short time or cooling of the TMG container. The surface chemistry for ALD of GaN from TMG has been extensively investigated using a variety of surface sensitive experimental and theoretical techniques[5,9,10,11,12].

In contrast, ALD of GaN from TEG has been less studied. Stegmuller *et al*,[13] have presented a quantum chemical study on the gas-phase decomposition pathways of TEG using density functional theory (DFT). They concluded that β-hydride elimination, *i.e.*, replacing one ethyl ligand with a hydrogen on the gallium center while forming ethylene, is the dominant gas-phase decomposition pathway for TEG in a thermal CVD process. In surface chemistry studies with TEG, ethyl groups are found to deposit onto the surface by the decomposition of TEG, followed by desorption at higher temperatures as ethylene (C_2H_4) and/or ethane (C_2H_6). This reaction has been shown on Ni(100)[14], GaAs(100)[15] and Si(100)[16]. For ALD of GaN, TEG adsorption and subsequent reactions are dependent on the surface termination after the NH_3 pulse. We have previously investigated equilibrium surface terminations after the NH_3 pulse on GaN(0001) and shown that $–NH_2$ was the main surface structure up to about 600K.[17]

In a previous study on ALD of GaN using TEG and NH_3 with and without plasma activation of ammonia,[18] we explored how the surface chemistry can enhance the elimination of the ethyl ligands by introducing a reactive B pulse of H_2, Ar plasma, or H_2-Ar plasma, between the TEG

and ammonia pulses. The results showed that adding a B-pulse afforded higher growth per cycle (GPC). We hypothesized that H_2 gas as a B pulse would favor H_2-assisted C_2H_6 elimination, Ar plasma would bring additional energy to the surface, favoring β-hydrogen elimination, while H_2-Ar-plasma as B pulse would favor both H_2-assisted C_2H_6 elimination and β-hydrogen elimination of C_2H_4. All these mechanisms would render a hydrogen-terminated surface with less steric hindrance than an ethyl-terminated surface.

Herein, we used quadrupole mass spectrometry (QMS) for real-time monitoring of GaN ALD from TEG and NH_3 with and without plasma activation to study the surface chemistry of the process. The previously proposed mechanisms for introducing a B-pulse were also experimentally investigated using a QMS.

II. EXPERIMENTAL DETAILS

The film deposition was carried out using a hot-wall Picosun R-200 Advanced ALD reactor, equipped with a Litmas remote inductively coupled plasma (ICP) source with a substrate holder located approximately 75 cm downstream from the plasma source, at an operating pressure of approximately 5 hPa. The TEG was maintained in a stainless-steel bubbler at room temperature. N_2 (99.999%) was used as purge gas for the deposition system and as a carrier gas for the TEG precursor, while Ar (99.9997%) was used as the carrier gas for H_2 (99.999 %) and NH_3 (AGA/Linde, 99.999 %) precursor delivery. The N_2, Ar, NH_3, and H_2 gases were further purified by getter filters. To study the deposited film after the experiments, a sample Si (100) piece (1.5×1.5 cm) was loaded in the reaction chamber and kept at the deposition temperature for 120 min before starting the growth process. It should be noted that the surface area of the chamber walls is much higher than that of the Si piece, and the measured reaction products mainly emanate from the chamber walls.

Following the ALD settings from our previous study, made in the same ALD reactor[18], in the standard ALD growth cycle (A-C cycle) used TEG was pulsed for 0.3 s followed by a 10 s N_2 purge, followed by a NH_3 pulse for 12 s using a mixture of 50 SCCM NH_3 and 100 SCCM Ar, followed by a 6 s purge. To study plasma-activated ALD, 2800 W plasma power was used. The same gas lines and NH_3/Ar flows were used for both the thermal and plasma processes. For A-B-C cycle experiments, 3 types of B pulses were introduced in a separate manner into the reaction chamber, a 12 s B-pulse of either Ar-plasma (100 SCCM with 2000 W plasma power), H_2 gas (50 SCCM H_2 mixed with 100 SCCM Ar), or H_2 plasma (50 SCCM H_2 mixed with

100 SCCM Ar and 2000 W plasma power) was added. A 2 s N_2 purge was added after each of the B-pulses.

A residual gas analysis (RGA) system was connected to the ALD reactor (located approximately 80 cm from the reaction chamber). The gaseous species and reaction byproducts were measured using a Hiden Analytical HPR-30 residual gas analysis (RGA) vacuum process sampling system that contains a HAL 201 RC mass spectrometer (MS) with a Faraday Cup detector. MS analysis involved collecting both scan spectra and multiple ion detection (MID) of specific ions with an electron impact ionization set at 70 eV, enabling the detection and analysis of gas-phase reaction products. The pressure in the QMS was maintained below 10^{-7} Torr using differential pumping with a turbomolecular pump. The ALD process used for the QMS measurements was modified by increasing all the purging times up to 90 seconds to have a better resolution in time of the ALD process. The data was then collected for a total flow of five cycles for both the A-C pulses and the A-B-C pulses prior to the collection of the RGA results. Prior to every measurement, the background signal of the reactor was measured in the range of mass-to-charge ratio (*m/z*) range from 1 to 100 to serve as a reference. The QMS measurements were performed with 200, 300, or 400 °C on the reactor walls and substrate holder.

III. RESULTS

Figure 1 shows the mass spectra collected when both the precursors were pulsed into the ALD reactor. The main *m/z* signals detected from the ALD reactor were 2, 14, 15, 16,17, 18, 20, 28, and 40, attributed to H_2, N, NH, NH_2, NH_3, Ar^{2+}, H_2O, N_2, and Ar, respectively. Notably, no other species were detected beyond *m/z*= 50. We note a problematic situation in that the *m/z* 28 peak can be attributed to both N_2^+, which is used to constantly purge all lines in the ALD reactor, and $C_2H_4^+$, which is the expected reaction product of β-elimination of the ethyl groups from TEG. The peak at *m/z* = 30, attributed to C_2H_6, *i.e.*, a protonated ligand appears solely when the reactants are injected into the ALD chamber, indicating that it is likely a surface reaction product. The peak observed around *m/z*= 29, attributed to an ethyl group C_2H_5, was significantly more intense when the precursors were introduced into the reactor, meaning it could emanate from precursor decomposition or surface reactions. We note that *m/z = 29* is also reported as a decomposition product of C_2H_6 in mass spectrometry, albeit with a reported intensity lower than that for *m/z* = 30[19], *i.e.*, the opposite relation than in Fig.1. From these

observations, the time-resolved measurements of thermal and plasma ALD were tracked as a function of C_2H_6 and C_2H_5 as indicators of surface reactions.

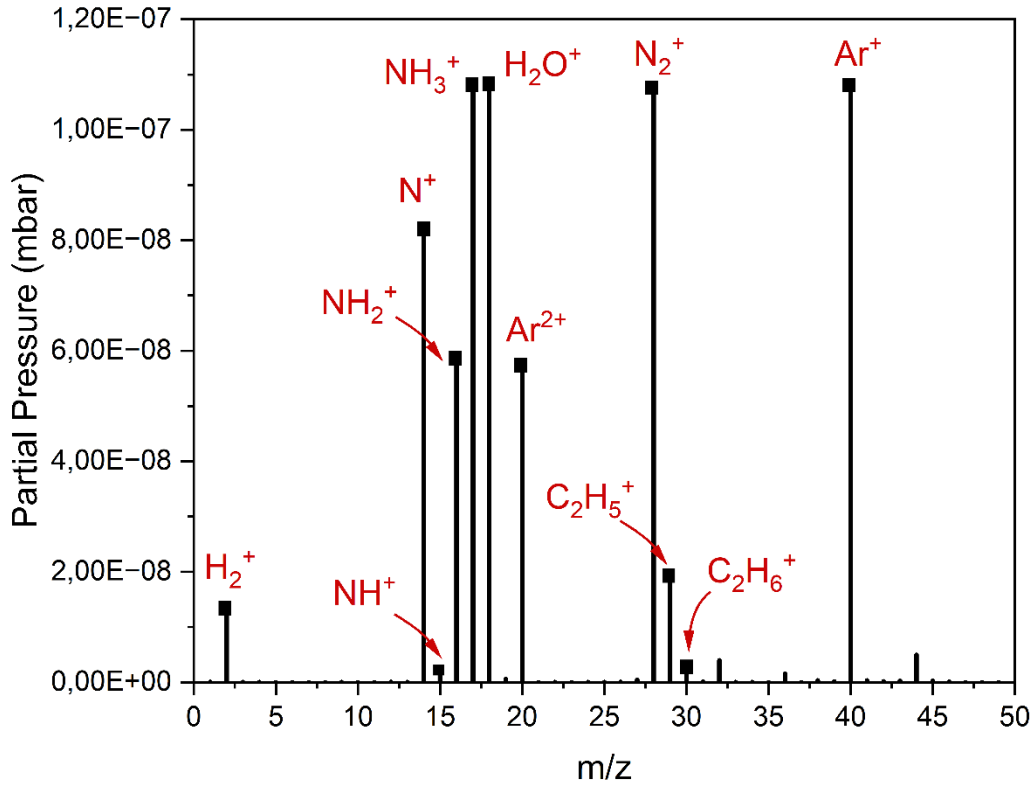

FIG. 1. *A survey scan showing average intensities of all detected masses during TEG: NH_3 (plasma) pulsed for 5 ALD cycles. Similar scans were obtained throughout all studied temperatures (200,300 and 400°C).*

Figure 2 shows the evolution of the signals from *m/z*= 29 and 30 during five ALD cycles with TEG and NH_3 plasma at 200, 300, and 400 °C. A spike in the *m/z* = 29 signal was observed both when TEG and NH_3 plasma were introduced into the chamber (Fig. 2a). This indicates the elimination of ethyl ligands during both precursor pulsing times. This is contrasted by the *m/z*= 30 signal, which spikes only during the NH_3 plasma, except when the temperature is 400 °C. This indicates that the hydrogen radicals produced in the ammonia plasma[20] promote ethane elimination.

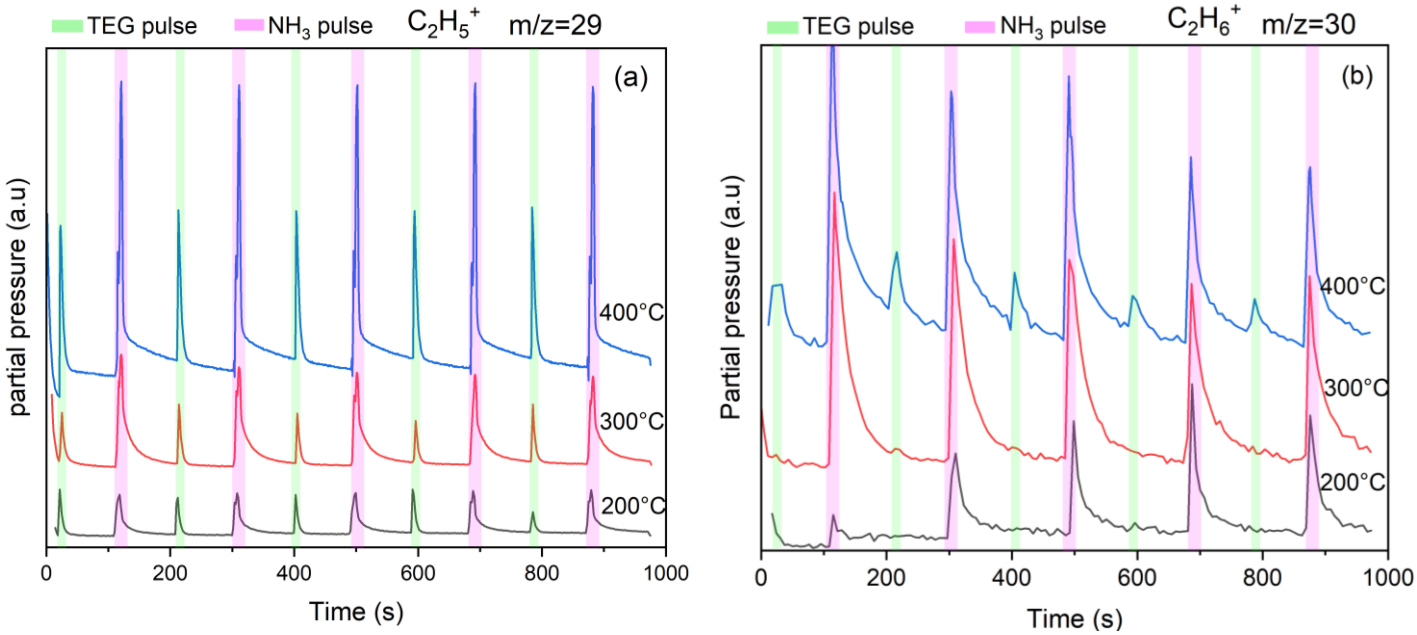

FIG. 2. *Time-resolved QMS data of m/z = 29 ($C_2H_5^+$) (a), and m/z = 30 ($C_2H_6^+$) (b), during sequential TEG and NH_3 plasma pulsing. The precursor dosing steps are alternated by nitrogen purge steps for 90 seconds.*

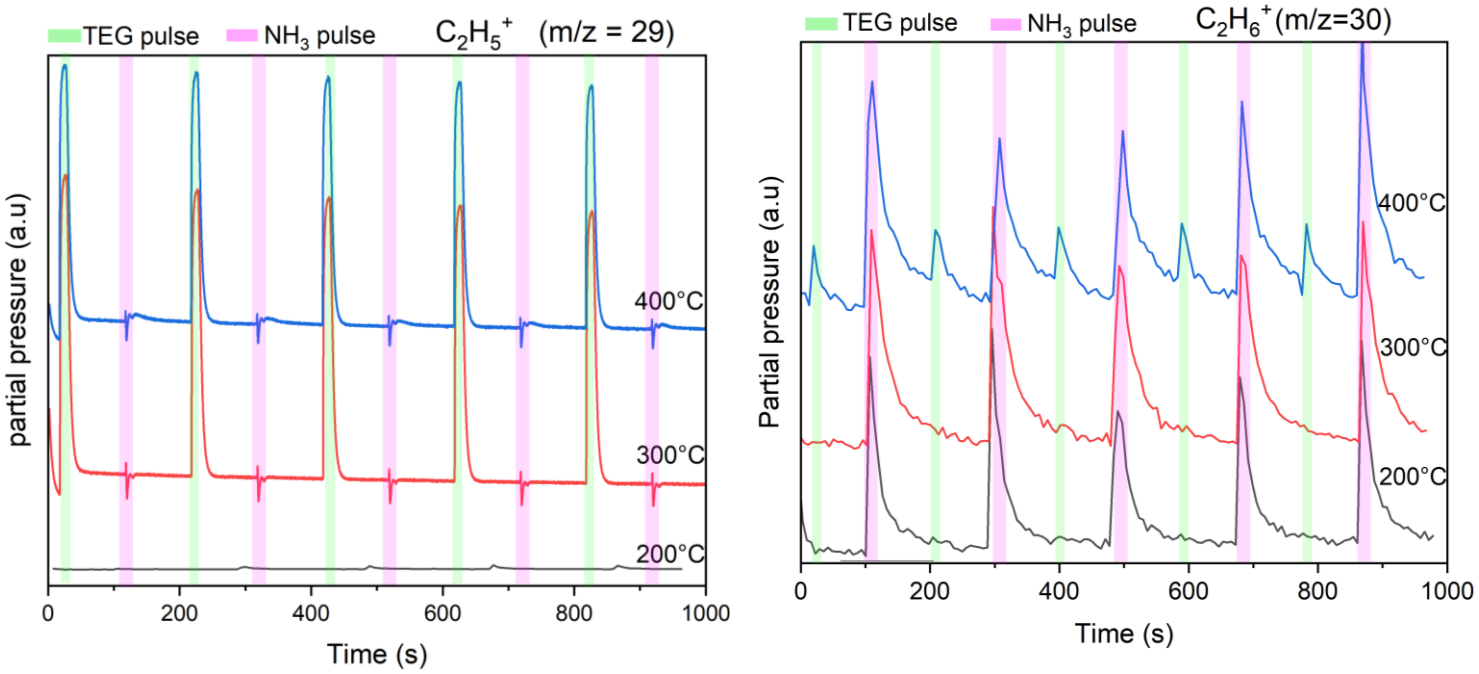

FIG. 3. *Time-resolved QMS data of m/z = 29 ($C_2H_5^+$) (a), and m/z = 30 ($C_2H_6^+$) (b) during sequential TEG and thermal NH_3 pulsing. The precursor dosing steps are alternated by nitrogen purge steps for 90 seconds.*

The thermal ALD process showed a different trend for *m/z* = 29 compared with the plasma process. No *m/z* = 29 signal was detected when ammonia was introduced into the reactor, whereas the intensity of the signal increased significantly when the TEG was pulsed at 300 and 400°C (Fig. 3a). The *m/z* = 30 signal showed similar results in the thermal and plasma processes with a spike only during the NH_3 pulse (Fig 3b).

IV. Discussion

A. TEG pulse

Since the *m/z* = 30 is expected to be higher than the *m/z* = 29 peak in the mass spectrum of C_2H_6[19], *i.e.*, the protonated ligand, we propose that the high intensity observed for *m/z* = 29 (Fig. 1) is explained by ethyl groups eliminated from the surface during the ALD process. We speculate that the dissociative adsorption of TEG, forming surface ethyl groups, could allow for the desorption of intact ethyl radicals (C_2H_5). According to the mass spectrometry results (Fig. 2a), the C_2H_5 signal is already fully developed at temperatures as low as 200°C and stays rather constant up to 400°C, suggesting that TEG could undergo dissociative adsorption at or above 200°C. Surface ethyl ligands can also desorb as ethane (C_2H_6) after reacting with surface hydrogen (Fig. 2b). As this reaction depends on the availability of a nearby surface hydrogen, it is reasonable to expect it to be less frequent, and a lower intensity for *m/z* = 30 (C_2H_6) compared to *m/z* = 29 (C_2H_5) is also noted in Fig. 1. We noted a higher intensity for the C_2H_6 signal at 400°C than at lower temperatures (Fig. 2b), which could be related to precursor decomposition. Stegmuller *et al*. 2014[13] studied the decomposition pathways of TEG using DFT, they concluded that the H_2 assisted elimination of C_2H_6 is thermodynamically favored for all three ethyl ligands at 400 °C. We note from our previous study on this ALD process that the upper limit of the temperature window where the surface chemistry is self-limiting, *i.e.*, the so-called ALD window, seems to be 325-350 °C. Thus, we expect very limited stability for any chemisorbed TEG at 400 °C.

It is worth mentioning that the C_2H_6 signal could also emanate from a β-hydride elimination reaction, by which C_2H_4 molecules desorb and combine with H_2 to form C_2H_6. This reaction pathway has been reported to be the main route for liberating ethylene C_2H_4 from Si(100) and GaAs surfaces.[21,22] Additionally, Qi An et al[23] examined the reaction mechanisms involved in GaN growth with TEG using ab initio quantum mechanics calculations and found out that both C_2H_4 formation by β -hydride elimination and direct desorption of C_2H_5 may occur in the GaN

growth process[19]. As described above, it was not possible to track the C_2H_4 ion signal at *m/z= 28* in our mass spectrometry experiments, as this signal coincides with the signal from N_2, used as a carrier gas and thus present in high concentrations.

From this, we suggest that TEG bonds to surface NH_2 groups, losing one or more ethyl ligands as intact species or recombining with adjacent hydrogen to desorb as ethane. The possibility of β-elimination of C_2H_4 cannot be excluded, as it has been found favored in the gas phase[13]. We note that the decomposition pattern of C_2H_4, results in *m/z* = 25, 26, and 27[24], and the absence of such peaks can be seen as a sign that C_2H_4 formation is low during the ALD process.

B. NH_3 plasma pulse

During the second half-cycle with NH_3, high-intensity signals were observed for C_2H_6 compared to the TEG pulse, suggesting that more of these species were produced in the NH_3 pulse than in the TEG pulse (Fig. 2b). Therefore, we suggest that ammonia molecules, or possibly NH_x species in the plasma process[20], undergo a ligand exchange with surface-bound Ga centers to form a Ga–N bond and eliminate C_2H_6 as a byproduct. This is consistent with the QMS observations (Fig. 2b). Additionally, C_2H_5, which shows a signal during the NH_3 pulse (Fig. 2a), possibly indicates the ongoing elimination of the ethyl groups due to the large amount of generated energetic species favoring ligand removal.

C. NH_3 thermal pulse

Our previous study on GaN ALD from TEG used plasma-activated ammonia as the N precursor. Attempts to use thermally activated NH_3 rendered very modest deposition of a film that was found to be mainly gallium oxide.[18] Here, we used QMS to study a possible thermal ALD process with TEG and NH_3. While it did not render any film for temperatures up to 400°C, we present mass spectra here to add to the process understanding. Mass spectrometry showed no C_2H_5 signal during the NH_3 pulse, suggesting a decreased reactivity of the surface Ga species toward the NH_3 half reaction. This means that less TEG can adsorb onto the surface after the NH_3 pulse, which is in line with the lower intensity of the *m/z* = 29 signal after each full ALD cycle as shown in Fig. 3a. Our results suggest that a thermal energy of up to 400 °C is not sufficient for the ligand exchange to occur when NH_3 is pulsed into the reactor, however, plasma activation is needed, in line with our previous results on InN ALD.[25]

Based on these observations, we sketch a growth mechanism between TEG and NH_3 in Fig. 4.

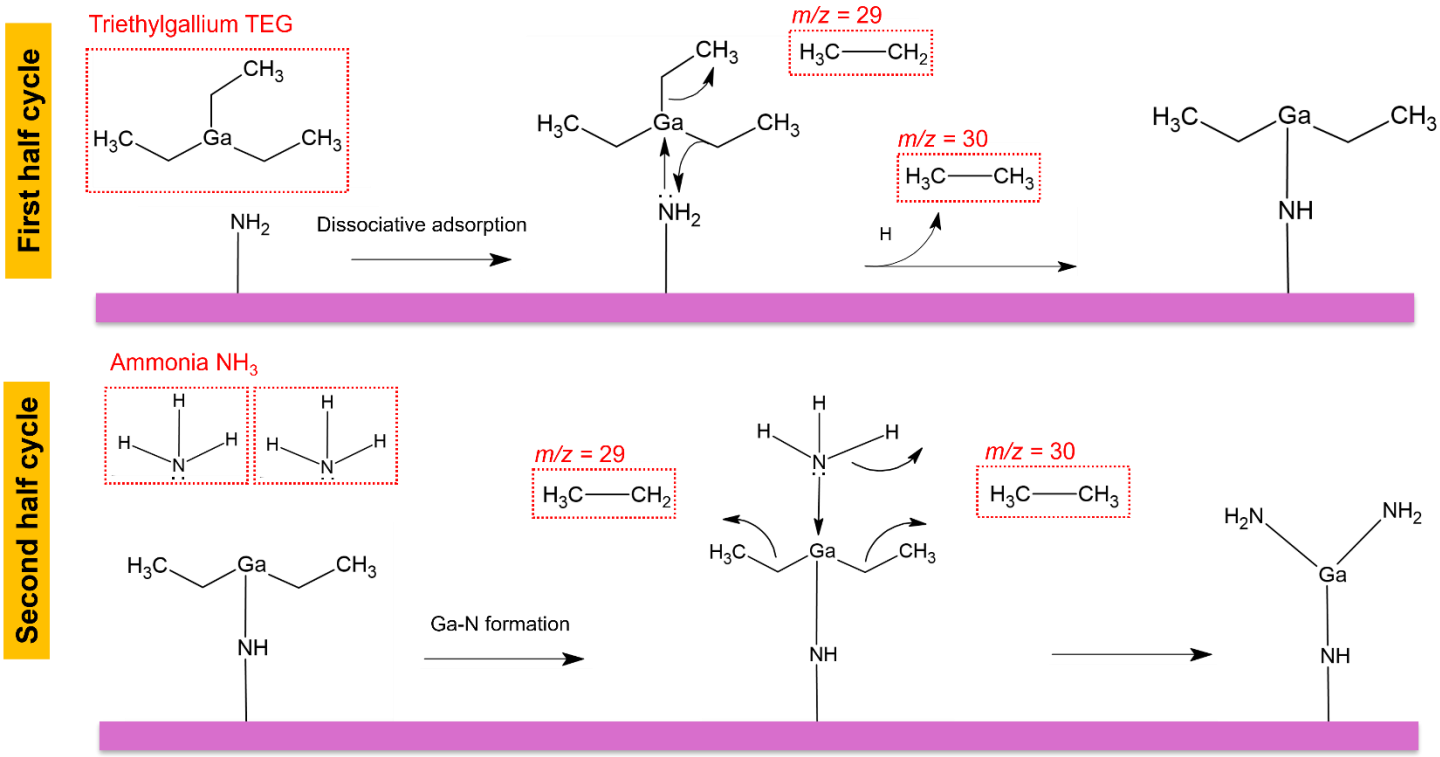

FIG. 4. *An illustration for the GaN film growth mechanism using sequential surface reactions between TEG and* NH_3.

D. Reactive B-pulse

As argued in our previous study, the addition of a reactive pulse (hydrogen plasma, hydrogen gas, and argon plasma) in between the precursor pulses improved the film quality and suggested to improve the removal of the ethyl ligands at an optimal temperature of 320°C during the plasma process. We used mass spectrometry to test this hypothesis and tracked the same *m/z* ratios 29 and 30 in Fig. 5.

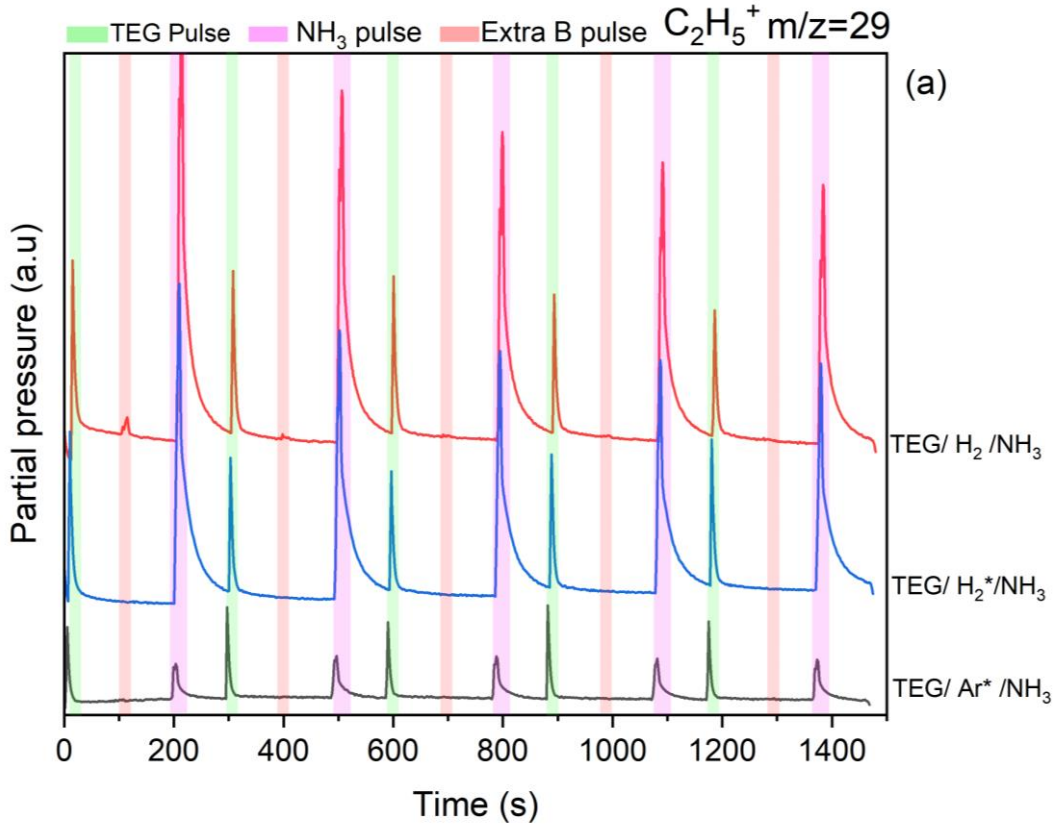

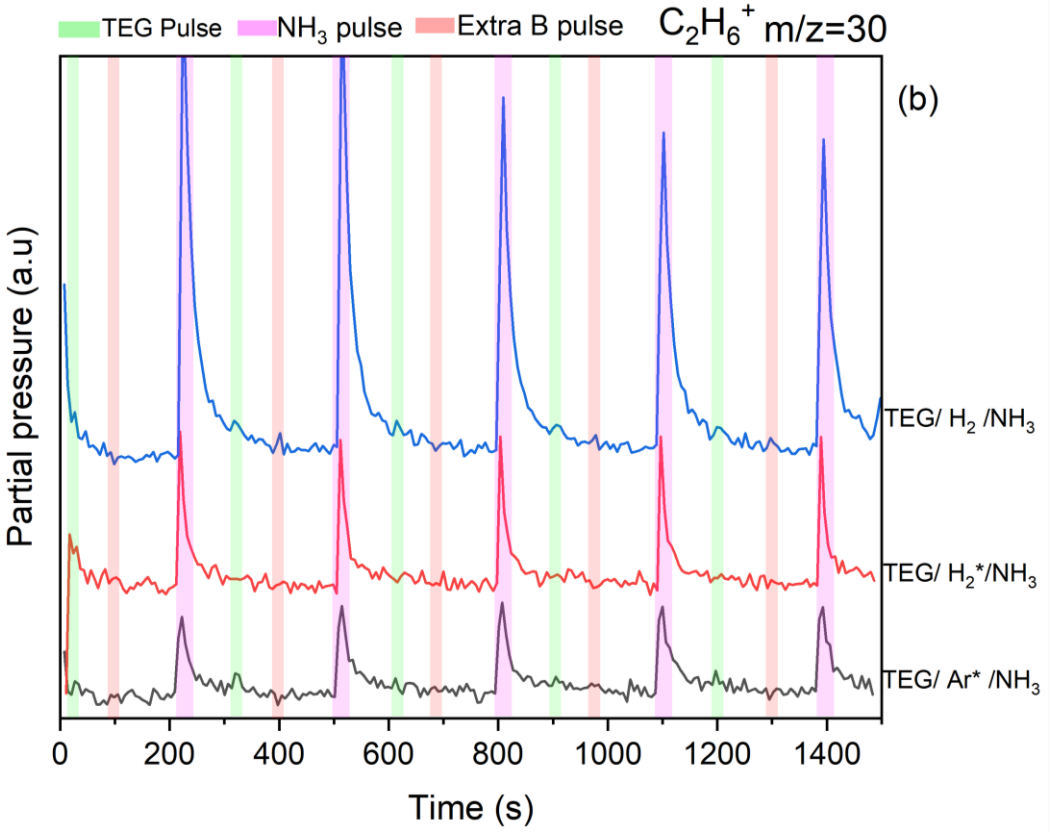

FIG. 5. *Time-resolved QMS data of m/z= 29 (C_2H_5) (a) and m/z 30 C_2H_6 (b) for plasma ALD of GaN when introducing the extra B pulse.*

The results show surprisingly no significant peaks when the extra pulses were introduced into the chamber, except for a slight increase in the peak signal for *m/z* = 29 with the hydrogen gas pulse, but lost intensity with time. Thus, we suggest that the B pulse does not favor ethyl elimination. Instead, we speculate that the observed increase in GPC in our previous study[18] is attributed to the B-pulse preparing the surface for subsequent nitridation by providing more time for the formation of more reactive or less sterically hindered intermediate(s).

V. SUMMARY AND CONCLUSION

Surface chemical reactions in the ALD of GaN from TEG and NH_3 plasma were experimentally examined using mass spectrometry. The reactions were monitored using *m/z* ratios of 29 and 30, corresponding to C_2H_5 and C_2H_6, respectively. We suggest that the TEG pulse resulted in a bond cleavage between the ethyl group and the surface, and the ethyl groups were removed either as intact ligands or through reductive elimination as ethane, thereby rendering diethylgallium on the surface. The second half of the reaction resulted in the formation of GaN monolayer formed by ligand exchange or hydrogenation reactions, releasing more ethyl ligands and rendering an NH_2 terminated surface.

ACKNOWLEDGMENTS

Formas (2022-00831) and the Swedish foundation for Strategic Research (SSF-RMA 15-0018) are gratefully acknowledged for financial support. HP acknowledge financial support from the Swedish Government Strategic Research Area in Mate-rials Science on Advanced Functional Materials at Linköping University (Faculty Grant SFO-Mat-LiU No. 2009-00971).

Conflicts of Interest

The authors have no conflict of interest to declare.

REFERENCES

[1] B.J. Baliga, Semicond. Sci. Technol. **28**, 074011 (2013).

[2] Y. Chen, J. Liu, K. Liu, J. Si, Y. Ding, L. Li, T. Lv, J. Liu, and L. Fu, Mater. Sci. Eng. R Reports **138**, 60–84 (2019).

[3] L.A. Reichertz, I. Gherasoiu, K.M. Yu, V.M. Kao, W. Walukiewicz, and J.W. Ager, Appl. Phys. Express **2**, 7–10 (2009).

[4] S.M. George, Chem. Rev. **110**, 111–131 (2010).

[5] S. Banerjee, A.A.I. Aarnink, D.J. Gravesteijn, and A.Y. Kovalgin, J. Phys. Chem. C **123**, 23214–23225 (2019).

[6] J.K. Sprenger, A.S. Cavanagh, H. Sun, K.J. Wahl, A. Roshko, and S.M. George, Chem. Mater. **28**, 5282–5294 (2016).

[7] M. Alevli, A. Haider, S. Kizir, S.A. Leghari, and N. Biyikli, J. Vac. Sci. Technol. A Vacuum, Surfaces, Film. **34**, 01A137 (2016).

[8] C. Ozgit, I. Donmez, and N. Biyikli, Acta Phys. Pol. A **120**, A-55-A-57 (2011).

[9] P. Pansila, K. Kanomata, M. Miura, B. Ahmmad, S. Kubota, and F. Hirose, Appl. Surf. Sci. **357**, 1920–1927 (2015).

[10] C.R. Flores, X.L. Zhou, and J.M. White, Surf. Sci. **261**, 99–110 (1992).

[11] N. Bahlawane, F. Reilmann, L.C. Salameh, and K. Kohse-Höinghaus, J. Am. Soc. Mass Spectrom. **19**, 947–954 (2008).

[12] T.R. Gow, R. Lin, and R.I. Masel, J. Cryst. Growth **106**, 577–592 (1990).

[13] A. Stegmüller, P. Rosenow, and R. Tonner, Phys. Chem. Chem. Phys. **16**, 17018–17029 (2014).

[14] S. Tjandra, and F. Zaera, Surf. Sci. **289**, 255–266 (1993).

[15] K.C. Wong, M.T. McEllistrem, B.G. McBurnett, R.D. Culp, A.H. Cowley, and J.G. Ekerdt, Surf. Sci. **396**, 260–265 (1998).

[16] D.-A. Klug, and C.M. Greenlief, J. Vac. Sci. Technol. A Vacuum, Surfaces, Film. **14**, 1826–1831 (1996).

[17] K. Rönnby, H. Pedersen, and L. Ojamäe, J. Phys. Chem. C **126**, 5885–5895 (2022).

[18] P. Deminskyi, C.-W. Hsu, B. Bakhit, P. Rouf, and H. Pedersen, J. Vac. Sci. Technol. A Vacuum, Surfaces, Film. **39**, 012411, (2021).

[19] N.M.S.D. Center, "NIST Chemistry WebBook, Ethane," (2014).

[20] P. Mpofu, H. Hafdi, P. Niiranen, J. Lauridsen, O. Alm, T. Larsson, and H. Pedersen, J. Mater. Chem. C **12**, 12818–12824 (2024).

[21] F. Lee, T.R. Gow, R. Lin, A.L. Backman, D. Lubben, and R.I. Masel, MRS Proc. **131**, 951–954 (1988).

[22] N.I. Buchan, and M.L. Yu, Surf. Sci. **280**, 383–392 (1993).

[23] Q. An, A. Jaramillo-Botero, W.G. Liu, and W.A. Goddard, J. Phys. Chem. C **119**, 4095–4103 (2015).

[24] N.M.S.D. Center, "NIST Chemistry WebBook, Ethylene," (2014).

[25] K. Rönnby, H. Pedersen, and L. Ojamäe, J. Vac. Sci. Technol. A **41**, 020401, (2023).